Tunable Fiber Bragg Grating Ring Lasers using Macro Fiber Composite Actuators

Demetris L. Geddis[a], Sidney G. Allison[b], and Qamar A. Shams[b]
[a]Department of Engineering, Norfolk State University, 700 Park Avenue, Norfolk, VA, USA 23504
[b]NASA Langley Research Center, Hampton, VA, USA 23681

ABSTRACT

The research reported herein includes the fabrication of a tunable optical fiber Bragg grating (FBG) fiber ring laser (FRL)[1] from commercially available components as a high-speed alternative tunable laser source for NASA Langley's optical frequency domain reflectometer (OFDR) interrogator, which reads low reflectivity FBG sensors. A Macro-Fiber Composite (MFC) actuator invented at NASA Langley Research Center (LaRC) was selected to tune the laser. MFC actuators use a piezoelectric sheet cut into uniaxially aligned rectangular piezo-fibers surrounded by a polymer matrix and incorporate interdigitated electrodes to deliver electric fields along the length of the piezo-fibers. This configuration enables MFC actuators to produce displacements larger than the original uncut piezoelectric sheet. The FBG filter was sandwiched between two MFC actuators, and when strained, produced approximately 3.62 nm of wavelength shift in the FRL when biasing the MFC actuators from –500 V to 2000 V. This tunability range is comparable to that of other tunable lasers and is adequate for interrogating FBG sensors using OFDR technology. Three different FRL configurations were studied. Configuration A examined the importance of erbium-doped fiber length and output coupling. Configuration B demonstrated the importance of the FBG filter. Configuration C added an output coupler to increase the output power and to isolate the filter. Only configuration C was tuned because it offered the best optical power output of the three configurations. Use of Plastic Optical Fiber (POF) FBG's holds promise for enhanced tunability in future research.

Keywords: Fiber laser, fiber Bragg grating, piezoelectric, actuator, tunable

1. INTRODUCTION

Optical FBG sensors can measure strain and other parameters such as temperature in numerous applications. Distributed FBG sensing is particularly beneficial for structural health monitoring applications such as Integrated Vehicle Health Management (IVHM) of aerospace vehicles [1-3]. Tunable lasers are widely used as a means of measuring gratings in optical fibers because they provide a variable wavelength output. A compact, lightweight, rapidly tunable laser compatible for use with the OFDR measurement system developed at NASA Langley Research Center (LaRC) [4] is needed for flight on spacecraft such as NASA's space shuttle, Reusable Launch Vehicle and Next Generation Launch Technology. The OFDR system can read out hundreds of low reflectivity FBG sensors distributed along the length of a single optical fiber [3].

Perhaps the most critical component in an OFDR is the widely tunable, mode-hop free, narrowband laser. Mode hopping creates discontinuities in the phase of the acquired signals, significantly degrading the recovered grating spectra. Over the past few years, the authors have used only two types of tunable lasers successfully in OFDR systems. The first type is the external cavity laser (ECL) diode. Several companies manufacture tunable ECL diodes but only a few have acceptable tuning characteristics. Mode hops typically are only suppressed over a limited part of the tuning range and high-speed jitter of the wavelength due to wavelength locking circuitry or other sources causes non-monotonic tuning.

[1] Work completed at NASA Langley during 2005 NASA Faculty Fellowship Program.

A second type of tunable laser is the stress-tuning erbium-doped optical fiber laser. This type was chosen for the research reported herein because fiber lasers can be designed with excellent mode-hop free tuning characteristics [5] needed for use with the OFDR system. Tunable fiber lasers offer additional advantages including narrow linewidth and ability to be rapidly tuned. Commercially available tunable lasers limit measurement frequency to 1 – 3 Hz repetition rate. The development of high-speed tunable erbium-doped fiber lasers can alleviate this drawback. FBG lasers can be tuned simply by applying a strain to the grating using a mechanical compressor, a piezoelectric actuator, a thin resistive coating, or an acoustooptic superlattice modulator. The paper examines three different FRL configurations. Configuration A examines the importance of erbium-doped fiber length and output coupling. Configuration B demonstrates the importance of the FBG filter. Configuration C adds an output coupler to increase the output power and to isolate the filter. Only configuration C was tuned because it offered the best optical power output of the three configurations.

2. BACKGROUND

2.1 Fiber ring lasers

There are two classes of fiber lasers; linear cavity type and ring cavity type. The ring cavity fiber lasers, also known as FRLs, have many advantages compared to linear fiber lasers including ease of single-mode operation, narrower linewidth, and higher output power. These along with other attractive attributes such as continuous wave or pulse operation, single longitudinal mode operation, and narrow linewidth have led to major research efforts to develop FRLs. Semiconductor ring lasers preceded FRLs and enlisted AlGaAs lasers with bulk lenses, mirrors, and beam splitters forming the feedback loop. The first FRL replaced the feedback loop with a semiconductor gain medium, a loop of highly birefringent fiber, and a tunable fiber directional coupler [6]. Substituting an optical fiber gain medium in place of the semiconductor gain medium further enhanced the FRL and led to the development of an all-FRL using an Nd^{3+}-doped single mode fiber ring resonator [7]. A closed ring was formed using a directional coupler.

The ring laser extended cavity configuration offers other advantages. It provides greater immunity to spurious external reflections, the ability to control the cavity loss and output power, and more importantly for tuning purposes, the structure for the insertion of filters and isolators. An optical bandpass filter with an Er^{3+} -doped FRL was incorporated demonstrating lasing wavelength tuning [8]. In addition, an electrically tunable Er^{3+} -doped FRL has been reported using fiber Fabry-Perot etalons instead of a passive optical filter [9].

Furthermore, using three port circulators and fiber couplers [10] allows FBG filters to be incorporated into FRLs. Fiber optic circulators are unidirectional devices that direct an optical signal (light) from one port to the next, in only one direction at a time. While the direction of the light may be redirected as needed, it must pass to and from ports sequentially (from port 1 to port 2 before traveling to port 3). A FBG filter is a periodic change of the index of refraction along a fiber, which is formed by exposure of the core of the fiber to a coherent ultraviolet (UV) light interference fringe pattern [11]. Figure 1 [12] illustrates FBG filter formation.

A FBG filter reflects only a narrow band of incident light due to successive coherent scattering from the index variation [11]. The strongest reflection occurs at the Bragg wavelength λ_B given by,

$$\lambda_B = 2n_{eff}\Lambda \qquad \textbf{Equation 1}$$

where n_{eff} is the modal index and Λ is the grating period [11]. The Bragg wavelength can be tuned by changing the modal index or the grating pitch. Tuning can be accomplished by strain, temperature, or polarization changes in the fiber.

Applying an axial or transverse strain shifts the Bragg wavelength of an FBG filter by dilating or compressing the grating and perturbing the effective index. The change in wavelength as a function of strain is given by,

$$\frac{\Delta\lambda_B}{\lambda_B} = \varepsilon_1 - \left(n^2/2\right)\left[p_{11}\varepsilon_t + p_{12}\left(\varepsilon_1 + \varepsilon_t\right)\right] \qquad \textbf{Equation 2}$$

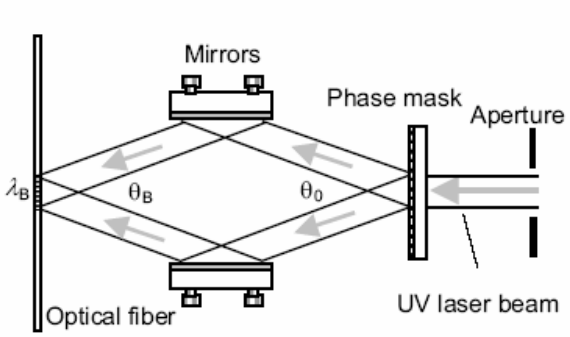

Figure 1: FBG filter fabrication process.

where ε_l is the principal strain along the fiber axis, ε_t is the principal strain transverse to the fiber axis, and p_{11} and p_{12} are the fiber Pockel's coefficients, which are related to photoelasticity of the fiber. When strain is uniform and homogeneous, the Bragg wavelength strain relationship can be approximated by,

$$\frac{\Delta\lambda_B}{\lambda_B} = \left(1 - p_e\right)\varepsilon \approx 0.78\varepsilon \qquad \textbf{Equation 3}$$

where p_e is the effective photoelastic constant, which is 0.22 for fused silica, and ε is the applied axial strain [11]. The strain-optic coefficient relating strain to normalized wavelength shift in equation 3 above is typically around 0.78. About 1 nm of wavelength shift is produced by 1000 microstrain at 1550 nm.

2.2 Macro fiber composite actuators

Typically, FBG filters are stretched and/or compressed with electro-mechanical devices such as translation stages or piezoelectric actuators. In the current research, the FBG filter is sandwiched between two Macro Fiber Composite (MFC) [13-16] piezoelectric actuators developed at NASA Langley. Their unique design makes these actuators very flexible as shown in the photograph in Figure 2 [13] allowing FBG filter sandwiching. Application of drive voltage to the pair of actuators strains the sandwiched FBG filter.

Figure 2: Flexible MFC actuator.

Figure 3 illustrates the primary components of a typical MFC actuator and their arrangement in an actuator. The MFC actuator consists of three primary components: 1) a sheet of aligned rectangular piezoceramic fibers, 2) a pair of thin polymer films each etched with a conductive electrode pattern and 3) an adhesive matrix material. The piezoelectric fiber sheets in the MFC are machined from low-cost piezoceramic wafers using a computer-controlled dicing saw. These sheets are easily handled and allow the piezoceramic fibers to be precisely aligned within the actuator package. Producing and handling the

piezoceramic fibers in precise groups reduces the production cost of the device. The fabrication technique is also precise and repeatable, and easily automated. The electrode pattern for the MFC is supported on a dielectric film, which serves both as an electrode carrier and an insulator. This baseline electrode pattern is typically produced using standard photoresist and-etched processes on commercially available copper-clad polyimide laminate film. The piezoceramic fibers are transferred from the carrier to film to the electrodes. Subsequent assembly consists of the application of an additional coat of adhesive to the fibers, placing the upper electrode film over the lower film, and curing the complete package under heat and pressure. This final consolidation step is typically performed in a vacuum press with heated platens. The MFC's design with rectangular piezofibers sandwiched between adhesives and electroded polyimide film makes the MFC actuator very durable. The microstrain per volt capability ranges from 0.5 to 1.2.

A completed LARC-MFC actuator is shown in Figure 4 [14-16]. The large rectangular pads, located at each end of the electrode bus lines, are tinned with solder prior to final lamination of the package. After lamination, the pads are heated to reflow the solder and form a permanent electrical connection between the top and bottom electrode bus lines. External electrical connections are easily made by removing a portion of dielectric film covering the pad, and soldering directly to the underlying copper layer. After assembly, a large, steady electrical field is applied to the actuator to pole the piezoceramic material. For an electrode finger spacing of 0.0042 inches, 3000 volts is sufficient to pole the PZT 5A type materials in a standard MFC actuator, with complete poling achieved in approximately 1 minute.

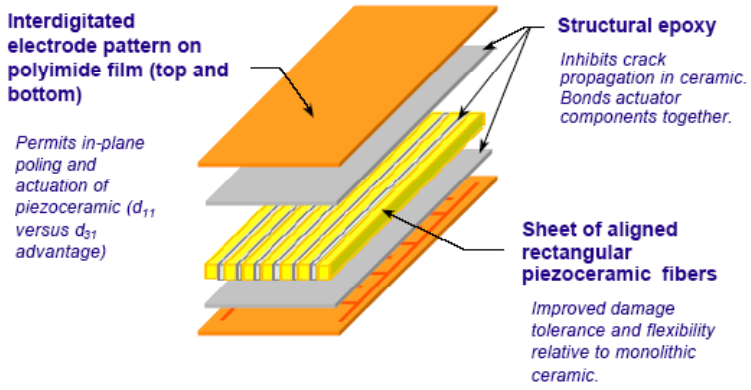

Figure 3: Primary components of a typical LaRC MFC actuator.

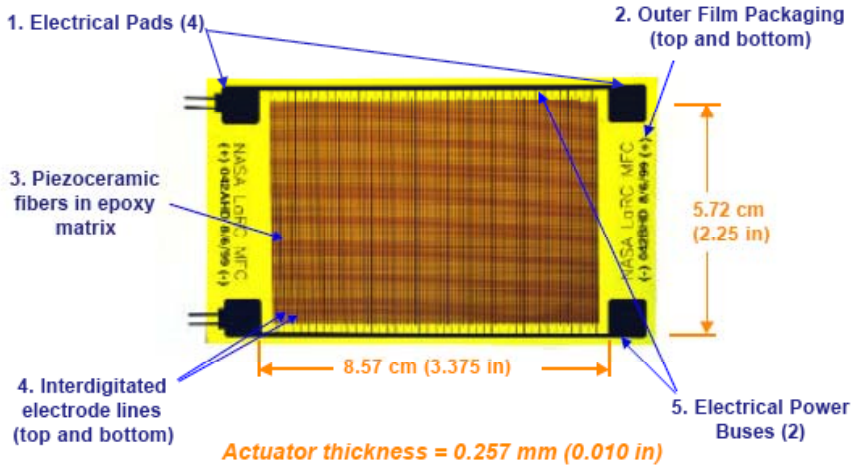

Figure 4: Completed MFC actuator.

3. TUNED FIBER BRAGG GRATING DESIGN

A schematic of a FBG sandwiched between two MFC actuators is shown in Figure 5. In this configuration an FBG based optical fiber is embedded between two finished MFC actuators using a vacuum bag process. Epoxy bonds the optical fiber to both actuators. Tunability of a MFC sandwiched FBG filter was previously reported [17]. This sandwich design, for which results are presented herein, is the best of three MFC fiber-straining designs examined in the previous work [17]. The two other MFC fiber-straining designs for which results are not presented herein were less successful. In the first approach, surface bonding, an optical fiber was simply bonded to the surface of an MFC using an adhesive. Before applying the adhesive, the surface of the MFC was roughened by sandblasting to improve the bonding. This design was non-symmetrical requiring a bend inhibitor and did not strain the fiber appreciably. In the second approach, embed bonding, a piezoelectric fiber was removed from a MFC actuator during its fabrication and replaced by a Bragg grating based optical fiber and the processing of the MFC was continued to completion with the optical fiber embedded in a single actuator. This fabrication process tended to break the optical fiber and was abandoned. An extension of the previous tunable filter work [17] is reported herein in which an MFC sandwich FBG filter is the tuning component of a tunable FRL.

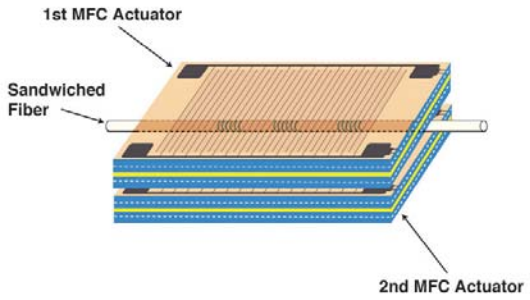

Figure 5: Schematic of a FBG sandwiched between two MFC actuators.

4. EXPERIMENTAL DESIGN-RING LASER CONFIGURATIONS

A photograph of the experimental setup is shown in Figure 6 for testing various diode pump MFC tunable ring laser configurations. The laser consisted of a 980 nm laser diode pump with drive current source, a wavelength division multiplexer (WDM), an erbium-doped fiber, a three port circulator, a FBG filter with a reflectivity >90% at 1550 nm sandwiched between two MFC actuators, and an output coupler. An optical spectrum analyzer measured the output spectrum of the FRL. To tune the laser, the MFCs were biased from –500 V to 2000 V using a standard power supply and a high voltage amplifier. The photoreceiver and multimeter measured optical output power.

The three FRL configurations shown in Figure 7 were tested to compare advantages and select the optimum circuit design. All three configurations used the pump laser, WDM, erbium-doped fiber, MFC sandwiched Bragg filter, and circulator. Configuration A incorporated a coupler and studied effects of erbium-doped fiber length and concentration. The circulator in this configuration acted as an isolator and the FBG filter did not influence the output spectrum. In configuration B, the coupler was removed, the circulator was connected properly, and output came from the FBG filter. This configuration demonstrated effectiveness of the FBG filter on wavelength selection. To increase the output power, a coupler was re-inserted into the loop as shown in configuration C. Most of the results reported are from configuration C because it produced higher power output than configuration B produced.

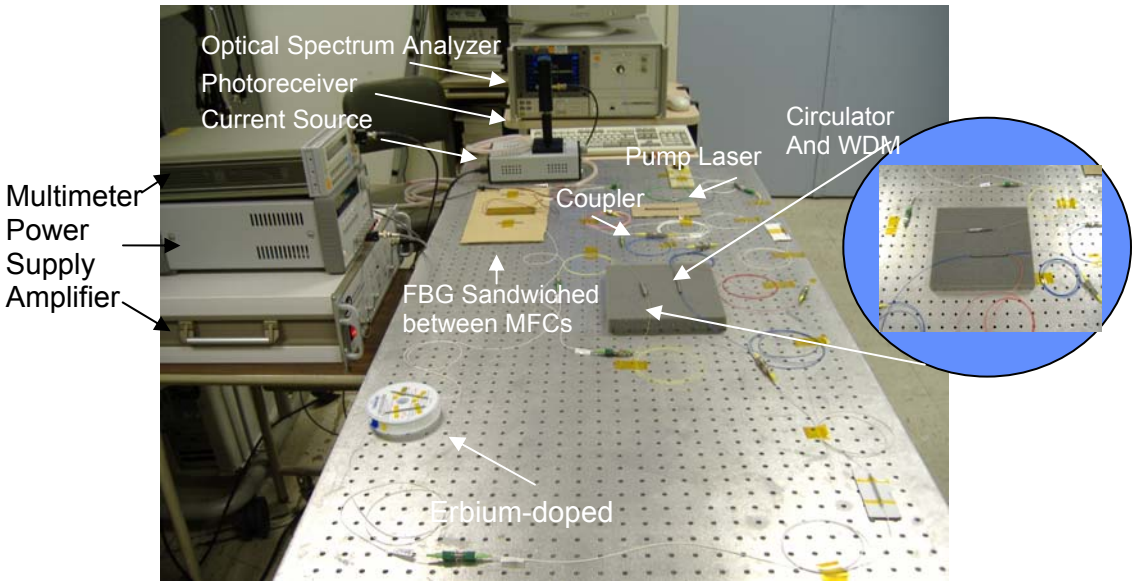

Figure 6: Experimental setup

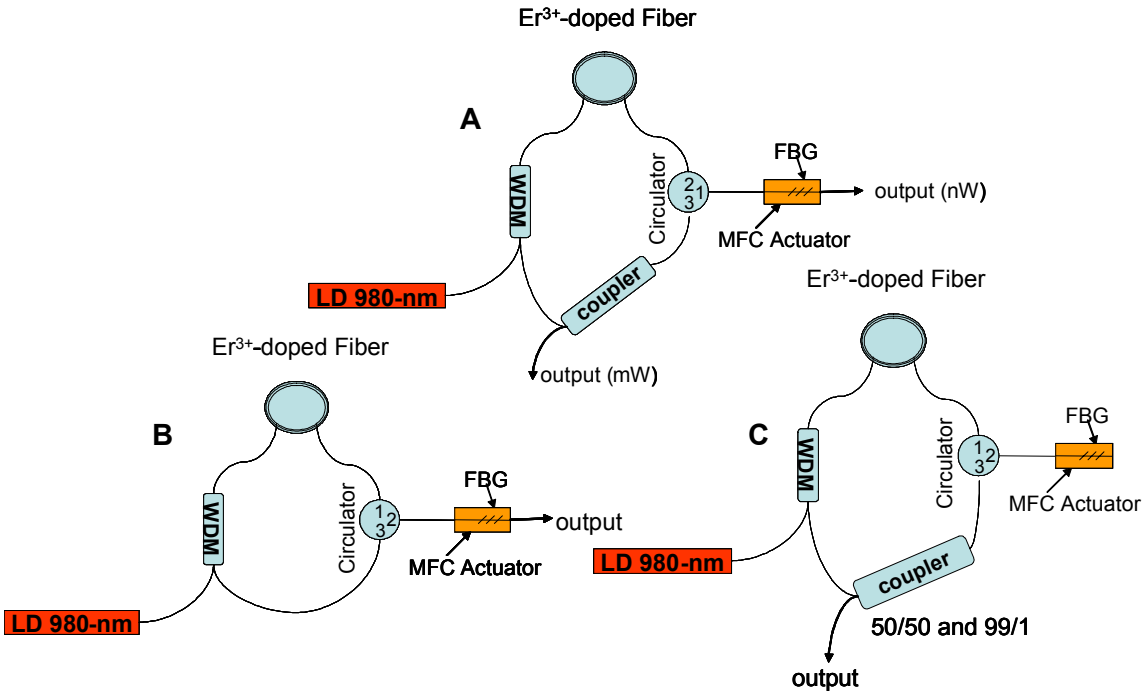

Figure 7: Schematics of FRL configurations in which circulator acts as isolator (A), FBG selects the wavelength (B), and coupler increases the output power (C).

5. EXPERIMENTAL RESULTS

Results from FRL configuration A are shown in Figure 8. Figure 8a shows results using a 99/1 coupler and Figure 8b shows results from a 50/50 coupler. These results reveal the effects of the output coupler on the number of modes that could lase for a given length of erbium-doped fiber. The 2 m long fiber's absorption was 23.4 dB/m at 980 nm and 37.20 dB/m at 1535 nm. With the 99/1 coupler the dominant mode was at a wavelength of 1571 nm. However, the 50/50 coupler supported a wavelength of 1562 nm. The wavelength selection was a function of the length of the fiber, type of coupler, and the erbium concentration. By changing the length of the erbium-doped fiber to 1 meter, a fiber with approximately the same erbium concentration lased at 1560 nm. As erbium concentration increased the wavelength increased. The 50/50 coupler reduced power making it more desirable for single wavelength tunable lasing.

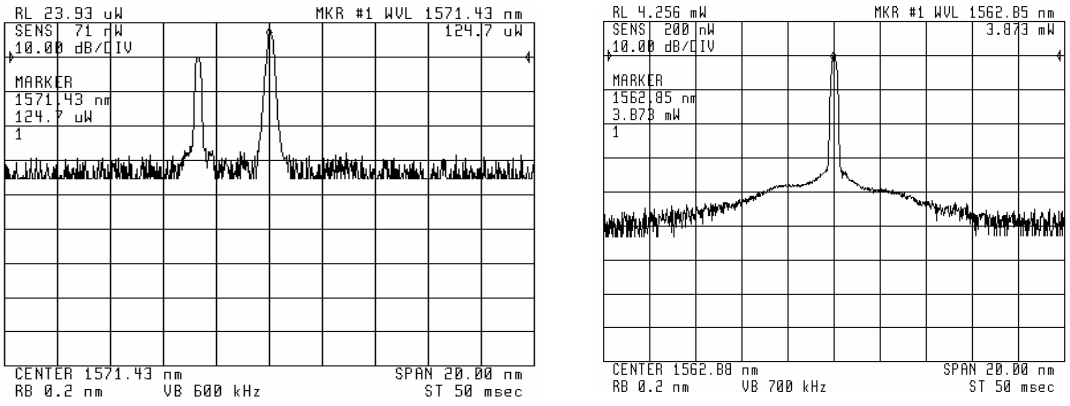

(a) (b)

Figure 8: Optical spectrum analyzer screen capture showing FRL optical output power amplitude (y-axis) vs. wavelength (x-axis). The FRL output shown in (a) resulted from using a 99/1 coupler and in (b) was achieved using a 50/50 coupler from configuration A.

By changing from FRL configuration A to configuration B, the effect of the FBG filter is shown in Figure 9. As expected the wavelength of 1550 nm was selected by the FBG. Configuration B incorporated the 50/50 coupler along with the 2 meter length of erbium-doped fiber from configuration A.

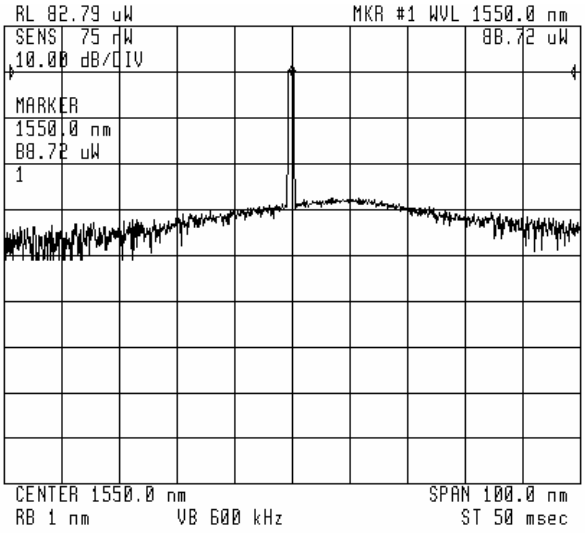

Figure 9: Optical spectrum analyzer screen capture showing FRL optical output power amplitude (y-axis) vs. wavelength (x-axis) from configuration B.

A schematic of the diode pumped MFC tunable FRL constructed with FRL configuration C is shown in Figure 10a and output spectrum of the FRL is shown in Figure 10b. Experimental results for configuration C are shown in Figure 11. The authors only tuned configuration C because it produced 10 times more output power than did configuration B making it of greater interest. Lasing began at a pump power of 14 mW with a slope efficiency of 1.8%. Figure 11a shows the wavelength shift of the laser as a function of applied voltage to the MFCs. The inherent hysteresis of piezoelectric material was seen when the voltage decreased from 2000 V to –500 V. The wavelength of the laser varied from 1549.38 nm to 1553 nm as shown in Figure 11b. This 3.62 nm shift is comparable to the tuning range of the predecessor tunable laser flown on space shuttle flight STS-96 for hydrogen leak detection [18], but the MFC hardware is much lighter weight and capable of more rapid tuning. Typical measurement fiber applications require the tunable laser to produce 3-15 nm wavelength shift [19] for gratings written at 1550 nm. The 3.60 nm wavelength shift achieved here may be adequate for OFDR applications where measurement fiber FBG sensors experience modest wavelength shifts due to small strains and minor temperature changes. Potential exists to increase FRL wavelength shift thereby expanding usefulness for OFDR applications in which measurement FBG sensors experience large wavelength shifts caused by high strain levels or large temperature changes such as in cryogenic applications. Future work to enhance tunability includes substituting plastic optical fiber (POF) Bragg gratings in place of glass Bragg gratings. The strain-optic coefficient of POF Bragg gratings is approximately twice that of fused silica Bragg gratings shown in equation 3, therefore the same strain level in POF will produce approximately twice the wavelength shift of glass Bragg gratings. Additional enhancement of wavelength shift may be possible because the lower elastic modulus of POF might allow the MFC actuators to produce larger strains than achievable with glass.

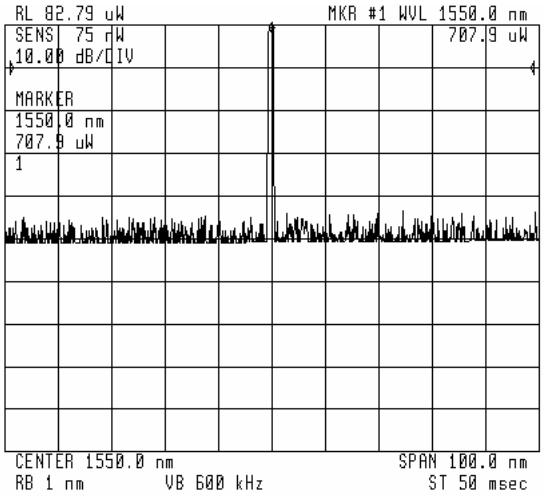

Figure 10: Optical spectrum analyzer screen capture showing FRL optical output power amplitude (y-axis) vs. wavelength (x-axis) from configuration C.

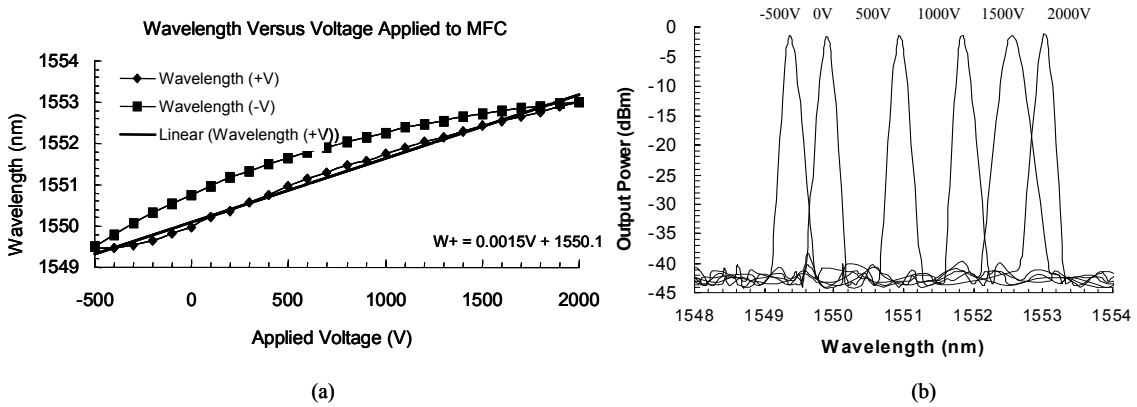

Figure 11: (a) Graph of wavelength versus voltage applied to the actuators and (b) optical spectra from configuration C.

6. CONCLUSIONS

Of the three FRL configurations studied, configuration 3 produced the highest optical power output making it of greater interest than the other two FRL configurations. Tuning of a fused silica FBG sandwiched between two MFC's using FRL configuration C produced adequate wavelength shift to be used as the tunable laser in an OFDR in applications where measurement FBG sensor wavelength shifts are small. Potential exists to increase FRL wavelength shift using POF instead of fused silica fiber thereby expanding usefulness for OFDR applications in which measurement FBG sensors experience large wavelength shifts caused by high strain levels or large temperature changes such as in cryogenic applications.

ACKNOWLEDGEMENTS

The authors gratefully acknowledge the programmatic support provided by Dr. Robert Rogowski of the Nondestructive Evaluation Sciences Branch at NASA Langley Research Center and the fabrication support provided by Benjamin M. Copeland, Jr. and Richard L. Chattin of the Technology Development and Integration Branch at NASA Langley Research Center.

REFERENCES

[1] W. H. Prosser, S. G. Allison, S. E. Woodard, R. A. Wincheski, E. G. Cooper, D. C. Price, A. Tessler and J. L. Spangler, "Structural Health Management for Future Aerospace Vehicles", The Second Australian Workshop on Structural Health Monitoring, Monash University Australia, December 16-17, 2004

[2] Prosser, W. H., Wu, M-C, Allison, S. G., DeHaven, S. L. and Ghoshal, A., "Structural Health Monitoring Sensor Development at NASA Langley Research Center", Proceedings of the International Conference on Computational & Experimental Engineering and Sciences (ICCES '03), Corfu, Greece, paper ID 149, July 25-29, 2003.

[3] B. A. Childers, M. E. Froggatt, S. G. Allison, T.C.Moore, D.A.Hare, C.F.Batten,, D.C.Jegley,"Use of 3000 Bragg grating strain sensors distributed on four eight-meter optical fibers during static load testing of a composite structure", Proceedings, SPIE's 8th Annual International Symposium on Smart Structures and Materials in Newport Beach, California, Vol. 4332, Paper No. 4332-17, March 2001

[4] M. E. Froggatt and J. Moore, "Distributed Measurement of Static Strain in an Optical Fiber with Multiple Bragg Gratings at Nominally Equal Wavelengths," *Appl. Opt.* , Vol. 37, No. 10, pp. 1741-1746 (1998).

[5] G. A. Ball and W. W. Morey, "Continuously tunable single-mode erbium fiber laser," Opt. Lett. Vol. 17, No. 6, pp. 1979 –1981, 1992.

[6] Jopson, R. M., Eisenstein, G., Whalen, M.S., Hall, K. L., Koren, U., and Simpson, J. R., "A 1.55-μm semiconductor-optical fiber ring laser," Appl. Phys. Lett., vol. 48, no. 3, pp. 204-206, 1986.

[7] Yue, C. Y., Peng, J. D., and Zhou, B. K., "Tunable Nd^{3+}-Doped Fibre Ring Laser," Electron. Lett., vol. 25, no. 2, pp. 101-102, 1989.

[8] Iwatsuki, K., Okamura, H., and Saruwatari, M., "Wavelength-Tunable Single- Frequency and Single-Polarisation Er-Doped Fibre Ring-Laser with 1.4kHz Linewidth," Electron. Lett., vol. 26, no. 24, pp. 2033-2035, 1990.

[9] Zyskind, J. L., Sulhoff, J. W., Stone, J., Digiovanni, D. J., Stulz, L. W., Presby, H. M., Piccirilli, A., and Pramayon, P. E., "Electrically Tunable, Diode-Pumped Erbium-Doped Fibre Ring Laser with Fibre Fabry-Perot Etalon," Electron. Lett. vol. 27, no. 21, pp. 1950-1951, 1991.

[10] Pan, J. J. and Shi, Y., "Tunable Er^{3+}-doped fibre ring laser using fibre grating incorporated by optical circulator or fibre coupler," Electron. Lett. vol. 31, no. 14, pp. 1164-1165, 1995.

[11] Hill, K. O. and Meltz, G., "Fiber Bragg Grating Technology Fundamentals and Overview," J. Lightwave Technol., vol. 15, no. 8, pp. 1263-1276, 1997.

[12] M.-C. Wu, W.H. Prosser, R. S. Rogowski, and S. L. DeHaven, "Using Dual-wavelength Fiber Bragg Gratings for Temperature and Strain Sensing at Cryogenic Temperature," 27th Airbreathing Propulsion Subcommittee, JANNAF, Colorado Springs, CO, December 2003.

[13] http://www.smart-material.com/ (July 28, 2006)

[14] R. B. Williams, G. Park, D. J. Inman, and W. K. Wilkie, "An Overview of Composite Actuators with Piezoceramic Fibers," Proceedings, Int. Modal Analysis Conference (IMAC-XX: Conference on Structural Dynamics), pp. 421-427, February 4-7, 2002, Los Angeles, California.

[15] W. K. Wilkie, R. G. Bryant, R. L. Fox, R. F. Hellbaum, ,J. W. High, A. Jalink, JR., B. D. Little, P. H. Mirick U.S. patent 6,629,341 "Method of Fabricating a Piezoelectric Composite Apparatus" (October 2003).

[16] J. W. High, W. K. Wilkie "Method of Fabricating NASA-Standard Macro-Fiber Composite Piezoelectric Actuators", NASA/TM-2003-212427, ARL-TR-2833, June 2003.

[17] S. G. Allison, Q. A. Shams, and D. L. Geddis, "Stretch-tuning optical fiber Bragg gratings using macro-fiber composite (MFC) piezoelectric actuators," Proceedings, SPIE Optics East, Boston, Massachusetts, Vol. 6004, Paper No. 60040C, October 2005.

[18] J. P. Moore, B. A. Childers, M. E. Froggatt, A. L. Cook, N. C. Coffee, L. J. Coen, J. K. Diamond, P. T. Huynh, E. M. Riley, S. K. Stover, K. G. Vipavetz, J. E. Wells, K. L. Woodman, C. D. Armistrong, J. S. Sirkis, Y. T. Peng, "An Overview of the Fiber Optic Sensing System for Hydrogen Leak Detection in the Space Shuttle Discovery on STS-96", OSA Proceedings Bragg Gratings, Photosensitivity and Poling in Glass Waveguides, Stuart FL, Sep. 23-25 (1999).

[19] Sidney G. Allison, Robert L. Fox, Mark E. Froggatt, and Brooks A. Childers, "Novel piezoelectric actuators for tuning an optical fiber Bragg grating", Optical Engineering journal, Vol. 41, No. 10, p. 2448-2455, October 2002